Electronic Supplementary Material (ESI) for Physical Chemistry Chemical Physics

Supplementary Information

Intra- and inter-monomeric transfers in the light harvesting LHCII complex: the Redfield-Förster picture

Vladimir Novoderezhkin, Alessandro Marin, Rienk van Grondelle

Table S1. Interaction energies M_{nm} (cm^{-1}) for the trimeric LHCII complex, calculated in the dipole-dipole approximation using the structural data of Liu et al. (2004). The effective transition dipoles for Chl *a* and Chl *b* are taken to be 4 and 3.4 debye, respectively.

	a602	a603	a610	a611	a612	b608	b609	b601'	a613	a614	a604	b605	b606	b607
a602	0	38.11	-11.39	9.69	15.83	-5.84	-19.25	-0.35	-4.96	0.69	6.42	-0.71	5.60	7.13
a603	38.11	0	12.97	-2.70	-0.76	6.72	96.66	-0.71	2.68	-6.70	-3.28	1.13	-8.89	1.23
a610	-11.39	12.97	0	-24.96	23.10	61.97	3.86	-4.20	7.21	-1.55	-4.18	1.61	-3.28	-0.14
a611	9.69	-2.70	-24.96	0	126.92	4.35	4.30	-0.88	-6.15	4.55	-3.80	1.33	-2.52	-2.78
a612	15.83	-0.76	23.10	126.92	0	-1.08	-2.57	1.41	-0.47	-0.18	4.67	-2.85	3.10	3.07
b608	-5.84	6.72	61.97	4.35	-1.08	0	36.07	5.82	-2.01	1.30	-2.76	-5.13	-4.99	-4.43
b609	-19.25	96.66	3.86	4.30	-2.57	36.07	0	38.15	-2.92	2.33	-7.28	-0.77	-0.16	-11.99
b601'	-0.35	-0.71	-4.20	-0.88	1.41	5.82	38.15	0	0.90	0.17	2.69	-2.26	2.72	0.30
a613	-4.96	2.68	7.21	-6.15	-0.47	-2.01	-2.92	0.90	0	-50.22	2.12	-1.40	1.47	2.20
a614	0.69	-6.70	-1.55	4.55	-0.18	1.30	2.33	0.17	-50.22	0	-3.42	0.37	-2.16	-3.25
a604	6.42	-3.28	-4.18	-3.80	4.67	-2.76	-7.28	2.69	2.12	-3.42	0	3.35	104.56	35.93
b605	-0.71	1.13	1.61	1.33	-2.85	-5.13	-0.77	-2.26	-1.40	0.37	3.35	0	29.71	-4.47
b606	5.60	-8.89	-3.28	-2.52	3.10	-4.99	-0.16	2.72	1.47	-2.16	104.56	29.71	0	59.38
b607	7.13	1.23	-0.14	-2.78	3.07	-4.43	-11.99	0.30	2.20	-3.25	35.93	-4.47	59.38	0
a602'	1.11	8.14	2.95	0.55	-0.69	0.08	-10.66	49.64	-1.20	-0.86	-0.90	0.66	-0.82	0.53
a603'	5.22	-6.53	-0.91	-1.21	1.29	-0.54	0.23	-5.89	-0.48	-0.91	2.56	-0.26	2.80	3.18
a610'	0.76	-2.05	-0.68	-0.36	0.51	0.54	2.25	-5.95	0.07	-0.01	0.54	0.06	0.25	-0.20
a611'	-0.51	-0.15	-1.13	-0.24	0.57	2.70	4.63	24.89	0.45	0.29	0.27	-0.32	-0.78	-0.85
a612'	-0.51	2.40	1.14	0.42	-0.29	-0.61	-3.19	9.13	-0.66	-0.07	-0.67	0.48	-0.36	-0.43
b608'	-1.15	1.32	0.50	0.44	-0.11	0.40	-0.23	2.78	-0.17	0.38	-0.71	0.22	-0.67	-0.66
b609'	-2.33	2.33	0.68	0.71	-0.41	0.42	-0.34	3.79	-0.17	0.43	-1.05	0.18	-0.99	-0.94
b601''	0.22	-1.45	-0.34	-0.09	0.35	0.46	0.89	-0.43	0.23	0.73	-0.25	0.16	-0.34	-0.59
a613'	-0.44	-4.36	-1.19	0.22	-0.93	0.38	5.24	-10.79	2.00	0.97	-1.08	-0.97	-0.89	8.18
a614'	-2.51	4.15	0.70	0.81	-0.76	0.74	-4.57	3.59	0.49	1.11	-3.91	3.43	-5.63	0.73
a604'	1.15	-0.50	-0.19	-0.30	-0.01	-0.59	-0.26	-2.51	-0.25	-0.68	0.87	-0.49	1.07	1.34
b605'	-0.34	0.50	0.22	0.17	-0.04	0.04	-0.23	0.77	-0.22	0.12	-0.29	0.07	-0.20	-0.20
b606'	1.17	-0.41	-0.23	-0.36	0.10	-0.41	-0.12	-1.87	-0.23	-0.66	0.80	-0.24	0.82	0.88
b607'	1.82	-0.97	-0.43	-0.56	0.20	-0.47	-0.00	-2.49	0.22	-0.68	1.21	-0.34	1.20	1.51
a602''	1.11	5.22	0.76	-0.51	-0.51	-1.15	-2.33	0.22	-0.44	-2.51	1.15	-0.34	1.17	1.82
a603''	8.14	-6.53	-2.05	-0.15	2.40	1.32	2.33	-1.45	-4.36	4.15	-0.50	0.50	-0.41	-0.97
a610''	2.95	-0.91	-0.68	-1.13	1.14	0.50	0.68	-0.34	-1.19	0.70	-0.19	0.22	-0.23	-0.43
a611''	0.55	-1.21	-0.36	-0.24	0.42	0.44	0.71	-0.09	0.22	0.81	-0.30	0.17	-0.36	-0.56
a612''	-0.69	1.29	0.51	0.57	-0.29	-0.11	-0.41	0.35	-0.93	-0.76	-0.01	-0.04	0.10	0.20
b608''	0.08	-0.54	0.54	2.70	-0.61	0.40	0.42	0.46	0.38	0.74	-0.59	0.04	-0.41	-0.47
b609''	-10.66	0.23	2.25	4.63	-3.19	-0.23	-0.34	0.89	5.24	-4.57	-0.26	-0.23	-0.12	-0.00
b601	49.64	-5.89	-5.95	24.89	9.13	2.78	3.79	-0.43	-10.79	3.59	-2.51	0.77	-1.87	-2.49
a613''	-1.20	-0.48	0.07	0.45	-0.66	-0.17	-0.17	0.23	2.00	0.49	-0.25	-0.22	-0.23	0.22
a614''	-0.86	-0.91	-0.01	0.29	-0.07	0.38	0.43	0.73	0.97	1.11	-0.68	0.12	-0.66	-0.68
a604''	-0.90	2.56	0.54	0.27	-0.67	-0.71	-1.05	-0.25	-1.08	-3.91	0.87	-0.29	0.80	1.21
b605''	0.66	-0.26	0.06	-0.32	0.48	0.22	0.18	0.16	-0.97	3.43	-0.49	0.07	-0.24	-0.34
b606''	-0.82	2.80	0.25	-0.78	-0.36	-0.67	-0.99	-0.34	-0.89	-5.63	1.07	-0.20	0.82	1.20
b607''	0.53	3.18	-0.20	-0.85	-0.43	-0.66	-0.94	-0.59	8.18	0.73	1.34	-0.20	0.88	1.51

Table S2. The site energies (cm^{-1}) determined in our previous models and in the present study. The energies correspond to purely electronic transitions, i.e. do not include a reorganization energy shift.

	Site energies*	Site energies**	Site energies***	Site energies****
a602	15160	15103	15087	15157
a603	15283	15222	15222	15287
a610	15073	15038	15038	15073
a611	15115	15100	15100	15112
a612	15097	15082	15082	15094
b608	15763	15728	15689	15761
b609	15721	15686	15597	15721
b601'	15890	15854	15849	15889
a613	15175	15140	15150	15174
a614	15264	15249	15249	15260
a604	15460	15410	15310	15460
b605	15679	15674	15681	15679
b606	15851	15796	15745	15850
b607	15712	15677	15635	15714

*) monomeric model, modified Redfield, fitting of OD/LD/FL and TA (ref 19)
**) trimeric model, modified Redfield fitting of OD/LD/FL only (ref 19)
***) trimeric model, modified Redfield, fitting of OD/LD/FL/CD and TA (ref 21).
****) trimeric model, modified Redfield- generalized Förster model with coupling cutoff 15 cm^{-1}, fitting of OD/LD/FL/CD and TA (present work).

Table S3. Parameters of the exciton states (energies and wavefunctions) and the rates of intra-monomeric and inter-monomeric transfers within LHCII trimer at 77K. All the values are averaged over disorder (with the assignment of every exciton state and every relaxation pathway in each realization). The averaged energies and participation values are shown for one monomeric subunit.

	Exciton states													
	$k1_1$	$k1_2$	$k2_1$	$k2_2$	$k2_3$	$k3_1$	$k3_2$	$k4_1$	$k5_1$	$k5_2$	$k6_1$	$k6_2$	$k6_3$	$k6_4$
	Energies of the zero-phponon transitions (cm^{-1})													
	14807	14927	14716	14769	15009	15293	15399	15340	14779	14919	14968	15147	15251	15430
	Square of wavefunction showing participation of the pigments in the exciton states													
a602	**0.7382**	0.1471	0.0163	0.0550	0.0431	0.0001	0.0003	0.0001						
a603	0.1434	**0.7475**	0.0057	0.0076	0.0512	0.0299	0.0124	0.0023						
a610	0.0625	0.0167	**0.5874**	**0.3229**	0.0024	0.0025	0.0053	0.0002						
a611	0.0223	0.0273	0.1801	**0.2833**	**0.4869**	0.0000	0.0000	0.0000						
a612	0.0243	0.0277	0.2058	**0.3281**	**0.4142**	0.0000	0.0000	0.0000						
b608	0.0009	0.0002	0.0045	0.0026	0.0000	0.3419	**0.6086**	0.0413						
b609	0.0085	0.0334	0.0003	0.0004	0.0023	**0.5972**	0.2726	0.0854						
b601'	0.0000	0.0002	0.0000	0.0000	0.0000	0.0283	0.1008	**0.8707**						
a613									**0.8009**	0.1989	0.0002	0.0000	0.0000	0.0000
a614									0.1991	**0.7998**	0.0010	0.0000	0.0000	0.0000
a604									0.0000	0.0013	**0.8555**	0.0829	0.0017	0.0586
b605									0.0000	0.0000	0.0826	**0.7069**	0.1942	0.0163
b606									0.0000	0.0000	0.0524	0.0386	0.1046	**0.8043**
b607									0.0000	0.0001	0.0082	0.1715	**0.6995**	0.1208
	Rates of the transfers k→k within first subunit (ps^{-1})													
$k1_1$	-3.0265	**2.3558**	0.1740	***1.0507***	0.7764	1.4008	0.6064	0.0820	*0.0210*	**0.0430**	**0.0173**	0.0053	0.0044	0.0317
$k1_2$	***1.0917***	-8.4372	0.0462	***0.8965***	**3.0699**	**3.4307**	1.1430	0.3136	0.0032	*0.0573*	0.0056	**0.0111**	**0.0294**	0.0071
$k2_1$	0.4075	**1.1924**	-14.2057	**20.3978**	**12.0034**	0.3551	0.6494	0.0349	**0.0340**	0.0169	0.0073	0.0033	0.0019	0.0039
$k2_2$	**1.4234**	**2.4231**	***13.8996***	-22.5313	**19.6381**	0.3037	0.4491	0.0235	0.0116	0.0163	**0.0162**	0.0066	0.0026	0.0090
$k2_3$	0.0928	***2.3586***	0.0859	0.1858	-35.5873	**0.5983**	0.1270	0.0171	0.0006	*0.0440*	0.0016	0.0031	0.0033	0.0046
$k3_1$	0.0109	0.1061	0.0001	0.0005	0.0991	-11.7482	**17.7385**	1.3241	0.0000	0.0000	0.0004	**0.0098**	**0.0338**	0.0150
$k3_2$	0.0001	0.0007	0.0000	0.0001	0.0004	4.9438	-30.2328	***8.9487***	0.0000	0.0000	0.0000	0.0034	0.0102	**0.1340**
$k4_1$	0.0000	0.0004	0.0000	0.0000	0.0002	0.7157	**9.5194**	-10.7438	0.0000	0.0000	0.0000	0.0027	0.0063	0.0039
$k5_1$	**0.0269**	0.0075	***0.0211***	0.0150	0.0119	0.0005	0.0008	0.0001	-0.6474	**6.4814**	0.0092	0.0009	0.0005	0.0008
$k5_2$	0.0190	**0.0533**	0.0010	0.0045	**0.0942**	0.0003	0.0017	0.0002	0.6462	-6.4948	**0.0211**	0.0042	0.0071	0.0123
$k6_1$	0.0036	0.0041	0.0003	0.0009	0.0029	0.0138	0.0119	0.0010	0.0012	0.0123	-0.1146	**0.2728**	**1.2577**	**7.5684**
$k6_2$	0.0003	0.0017	0.0000	0.0001	0.0015	0.0167	0.0143	0.0089	0.0000	0.0010	0.0410	-6.6458	**7.1124**	**5.8314**
$k6_3$	0.0000	0.0012	0.0000	0.0000	0.0008	**0.0427**	**0.0385**	0.0129	0.0000	0.0001	0.0410	***5.8850***	-9.8854	**7.9379**
$k6_4$	0.0000	0.0000	0.0000	0.0000	0.0000	0.0021	*0.1185*	0.0058	0.0000	0.0000	0.0023	0.4828	1.5077	-21.3508
	Rates of the transfers k→k' from the first to the second subunit (ps^{-1})													
$k1_1$'	**0.0482**	**0.1595**	0.0033	0.0082	0.0074	**0.0712**	**0.0802**	**0.5603**	0.0014	0.0001	0.0020	0.0006	0.0003	0.0015
$k1_2$'	0.0184	0.0131	0.0002	0.0027	0.0044	0.0237	0.0217	0.1349	0.0007	0.0005	0.0026	0.0011	0.0025	**0.0056**
$k2_1$'	0.0018	0.0030	0.0010	0.0016	0.0001	0.0005	0.0009	0.0207	0.0005	0.0000	0.0002	0.0001	0.0000	0.0000
$k2_2$'	0.0064	0.0172	0.0020	0.0037	0.0006	0.0048	0.0056	**0.0641**	0.0009	0.0000	0.0005	0.0002	0.0000	0.0001
$k2_3$'	0.0020	0.0107	0.0000	0.0001	0.0039	**0.0302**	**0.0404**	**0.6446**	0.0000	0.0001	0.0002	0.0004	0.0006	0.0019
$k3_1$'	0.0000	0.0000	0.0000	0.0000	0.0000	0.0000	0.0001	0.0003	0.0000	0.0000	0.0000	0.0000	0.0000	0.0001
$k3_2$'	0.0000	0.0000	0.0000	0.0000	0.0000	0.0002	0.0003	0.0029	0.0000	0.0000	0.0000	0.0000	0.0000	0.0009
$k4_1$'	0.0000	0.0000	0.0000	0.0000	0.0000	0.0000	0.0004	0.0003	0.0000	0.0000	0.0000	0.0000	0.0001	0.0007
$k5_1$'	0.0015	0.0119	0.0010	0.0013	0.0004	0.0034	0.0049	0.0194	**0.0075**	0.0004	**0.0070**	**0.0086**	**0.0263**	0.0007
$k5_2$'	0.0146	**0.0436**	0.0000	0.0010	0.0048	0.0184	0.0078	0.0213	0.0000	0.0006	**0.0053**	**0.0118**	0.0043	**0.0125**
$k6_1$'	0.0002	0.0001	0.0000	0.0000	0.0000	0.0001	0.0001	0.0020	0.0000	0.0001	0.0001	0.0003	0.0004	0.0007
$k6_2$'	0.0000	0.0000	0.0000	0.0000	0.0000	0.0001	0.0001	0.0014	0.0000	0.0000	0.0000	0.0001	0.0002	0.0007
$k6_3$'	0.0000	0.0000	0.0000	0.0000	0.0000	0.0002	0.0001	0.0024	0.0000	0.0000	0.0000	0.0001	0.0004	0.0016
$k6_4$'	0.0000	0.0000	0.0000	0.0000	0.0000	0.0002	0.0005	0.0036	0.0000	0.0000	0.0000	0.0001	0.0002	0.0047
	Rates of the transfers k→k'' from the first to the third subunit (ps^{-1})													
$k1_1$''	**0.0385**	**0.0473**	0.0008	0.0048	0.0111	0.0002	0.0013	0.0001	0.0010	**0.0313**	0.0008	0.0005	0.0010	0.0013
$k1_2$''	**0.0615**	0.0157	0.0003	0.0072	0.0259	0.0001	0.0005	0.0006	0.0022	**0.0504**	0.0002	0.0002	0.0002	0.0001
$k2_1$''	0.0056	0.0021	0.0011	0.0027	0.0001	0.0000	0.0000	0.0000	0.0019	0.0003	0.0000	0.0000	0.0000	0.0000
$k2_2$''	0.0103	0.0069	0.0014	0.0037	0.0007	0.0000	0.0001	0.0000	0.0015	0.0026	0.0001	0.0001	0.0001	0.0001
$k2_3$''	0.0008	0.0019	0.0000	0.0000	0.0031	0.0000	0.0001	0.0001	0.0000	0.0015	0.0000	0.0000	0.0001	0.0000
$k3_1$''	0.0001	0.0010	0.0000	0.0000	0.0013	0.0000	0.0003	0.0001	0.0000	0.0002	0.0000	0.0001	0.0001	0.0006
$k3_2$''	0.0000	0.0001	0.0000	0.0000	0.0001	0.0000	0.0002	0.0003	0.0000	0.0000	0.0000	0.0000	0.0000	0.0002
$k4_1$''	0.0002	0.0014	0.0000	0.0000	0.0042	0.0002	0.0050	0.0005	0.0000	0.0000	0.0000	0.0005	0.0013	**0.0100**
$k5_1$''	0.0015	0.0022	0.0003	0.0008	0.0001	0.0000	0.0000	0.0001	**0.0071**	0.0001	0.0002	0.0000	0.0000	0.0001
$k5_2$''	0.0001	0.0006	0.0000	0.0000	0.0001	0.0000	0.0001	0.0002	0.0002	0.0005	0.0001	0.0001	0.0001	0.0002
$k6_1$''	0.0006	0.0014	0.0000	0.0000	0.0004	0.0000	0.0001	0.0001	0.0011	0.0028	0.0001	0.0001	0.0002	0.0003
$k6_2$''	0.0001	0.0002	0.0000	0.0000	0.0001	0.0000	0.0001	0.0001	0.0002	0.0013	0.0001	0.0001	0.0002	0.0007
$k6_3$''	0.0000	0.0001	0.0000	0.0000	0.0001	0.0001	0.0001	0.0002	0.0001	0.0002	0.0000	0.0001	0.0004	0.0010
$k6_4$''	0.0000	0.0000	0.0000	0.0000	0.0000	0.0000	0.0007	0.0004	0.0000	0.0000	0.0000	0.0001	0.0003	0.0049

*notice that we include the b601' pigment into the first monomeric subunit, thus considering the *b*608-609-601' trimer as a single strongly coupled cluster.

Table S4. Time constants of energy migration between the stromal- and lumenal-side Chl *a*-clusters. The effective time constants are shown (corresponding to transfers from the exciton states to the whole clusters). The estimation is based on the data from Table S3.

Donor state	Acceptor states	Time constant, ps
$k5_1$(*a*613)	$k1_1$, $k1_2$ (*a*602-603)	41.2
$k5_1$(*a*613)	$k2_1$, $k2_2$, $k2_3$ (*a*610-611-612)	21.6
$k5_1$(*a*613)	$k1_1$,$k1_2$,$k2_1$,$k2_2$,$k2_3$	14.2
$k5_2$(*a*614)	$k1_1$, $k1_2$ (*a*602-603)	9.9
$k5_2$(*a*614)	$k2_1$, $k2_2$, $k2_3$ (*a*610-611-612)	12.9
$k5_2$(*a*614)	$k1_1$,$k1_2$,$k2_1$,$k2_2$,$k2_3$	5.6
$k1_1$(*a*602)	$k5_1$, $k5_2$ (*a*613-614)	19.5
$k1_2$(*a*603)	$k5_1$, $k5_2$ (*a*613-614)	16.5
$k2_1$(*a*610)	$k5_1$, $k5_2$ (*a*613-614)	45.0
$k2_2$(*a*610-611-612)	$k5_1$, $k5_2$ (*a*613-614)	51.0
$k2_3$(*a*611-612)	$k5_1$, $k5_2$ (*a*613-614)	9.4

Table S5. Time constants of energy migration from *a*602-603 to the *a*602'-603' and *a*602"-603" clusters

	$k1_1$ (*a*602)	$k1_2$ (*a*603)
$k1_1'$ (*a*602')	20.7 ps	6.3 ps
$k1_2'$ (*a*603')	54.3 ps	76.3 ps
$k1_1''$ (*a*602")	26.0 ps	21.1 ps
$k1_2''$ (*a*603")	16.3 ps	63.7 ps

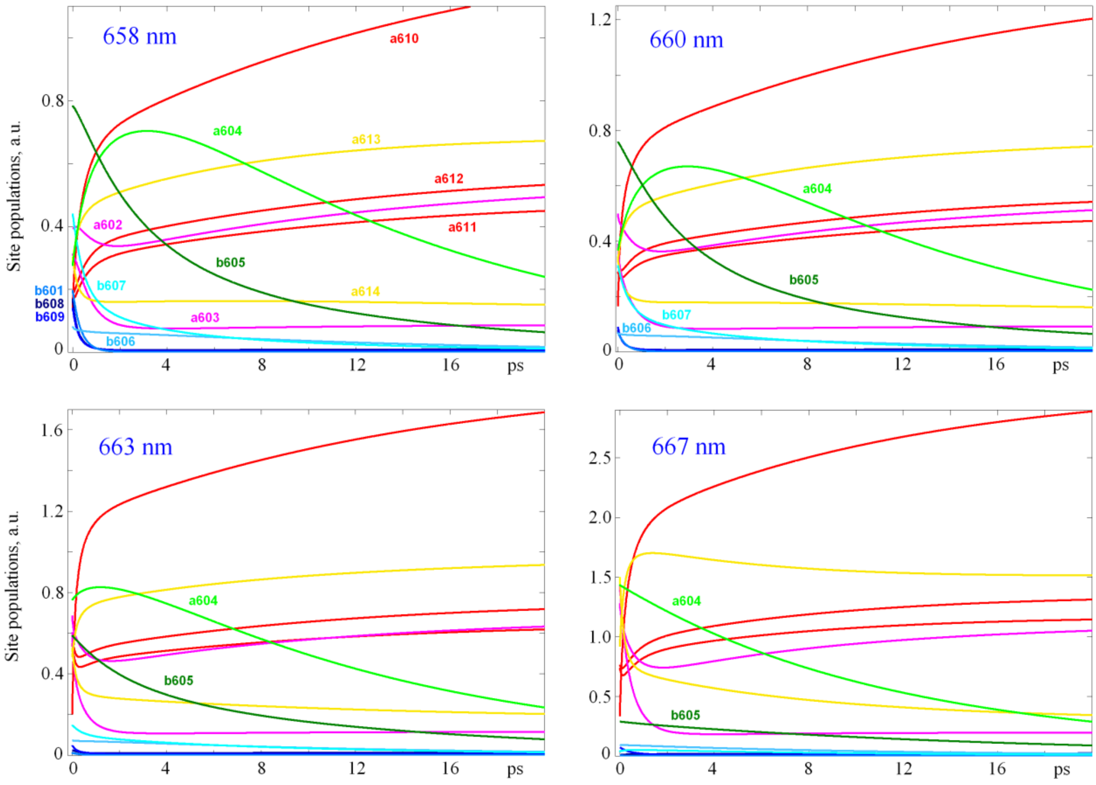

Figure S1. Site populations upon 658, 660, 663, 667 nm excitation. The total excited state population is wavelength-dependent, reflecting variation of the optical density at the excitation wavelength. Population dynamics of the 14 Chl sites is shown in the 0-20 ps scales. This dynamics is the same for each of the three monomeric subunits due to averaging over disorder.

The *b*605 (dark green) and *a*604 (light green) sites decay with components of 3.5-5 ps and 14-20 ps, respectively. The b605 contribution has a maximal amplitude upon 658 nm excitation (at 656 nm excitation its amplitude is lower than for 658 nm (data not shown)). The amplitude of the second component is increasing (with respect to the first one) when tuning the excitation from 660 to 667 nm (as indicated in Figure S1). Further tuning to the red, i.e. deeper into the Chl *a* region (>667 nm) is accompanied by a decrease of its amplitude. Notice that the big value of the *a*604 population upon 651 nm excitation (shown in Figure 6) is the result of fast *b*606→*a*604 relaxation, that is absent when tuning the excitation to the red of 651 nm.

We remind, that the 661 nm excitation of the LHCII trimers resulted in a long-lived shoulder in the 660-670 nm region decaying with time constants of 2.4 ps and 12 ps.[9] The second component becomes more pronounced upon tuning the excitation further to the red. Upon 672 nm excitation the 18 ps decay is observed.[9] Similar dynamics has been measured in the isolated LHCII monomers upon 663-669 nm excitation.[12] The two long-lived components observed in the intermediate region can be assigned (according to the present analysis) to the *b*605 and *a*604 sites.

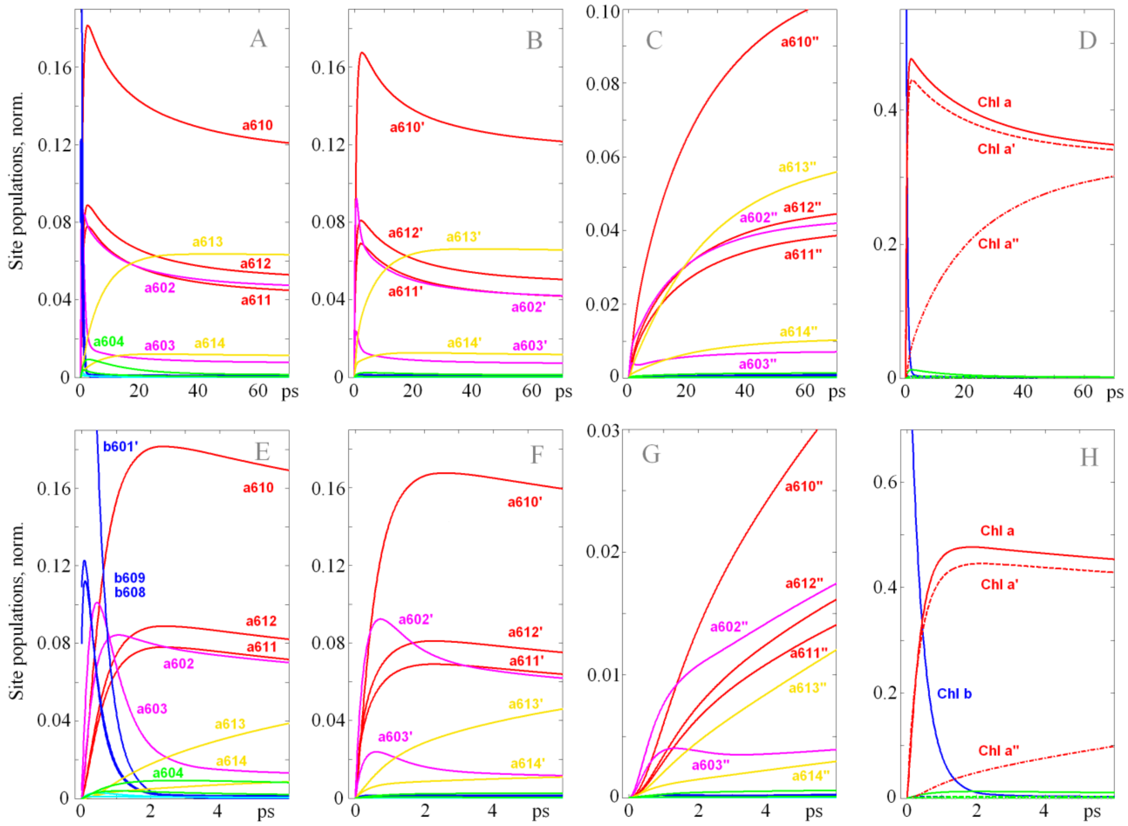

Figure S2. The same as in Figure 7, but for predominant excitation of *b*601' (with the averaged initial values of 0.81, 0.11, and 0.08 for the *b*601', *b*609 and *b*608 sites, respectively). Note the same y-scale in the A,E and B,F frames, that is different from the scale of the C,G frames corresponding to the third subunit.

Initial population of *b*601' (Figure S2) produces almost equal populations of the first and second subunits (as was discussed in the Section 4.2). This is in contrast with the case of *b*608 excitation, with predominant (80%) population of the first subunit during 1 ps and only 20% transfer to the second subunit via *b*601'. Population of the third subunit via *b*601' excitation exhibits almost the same dynamics as in the case of *b*608 excitation (compare frames (C,G) in Figures 7 and S2 showing almost identical kinetics for all the sites).

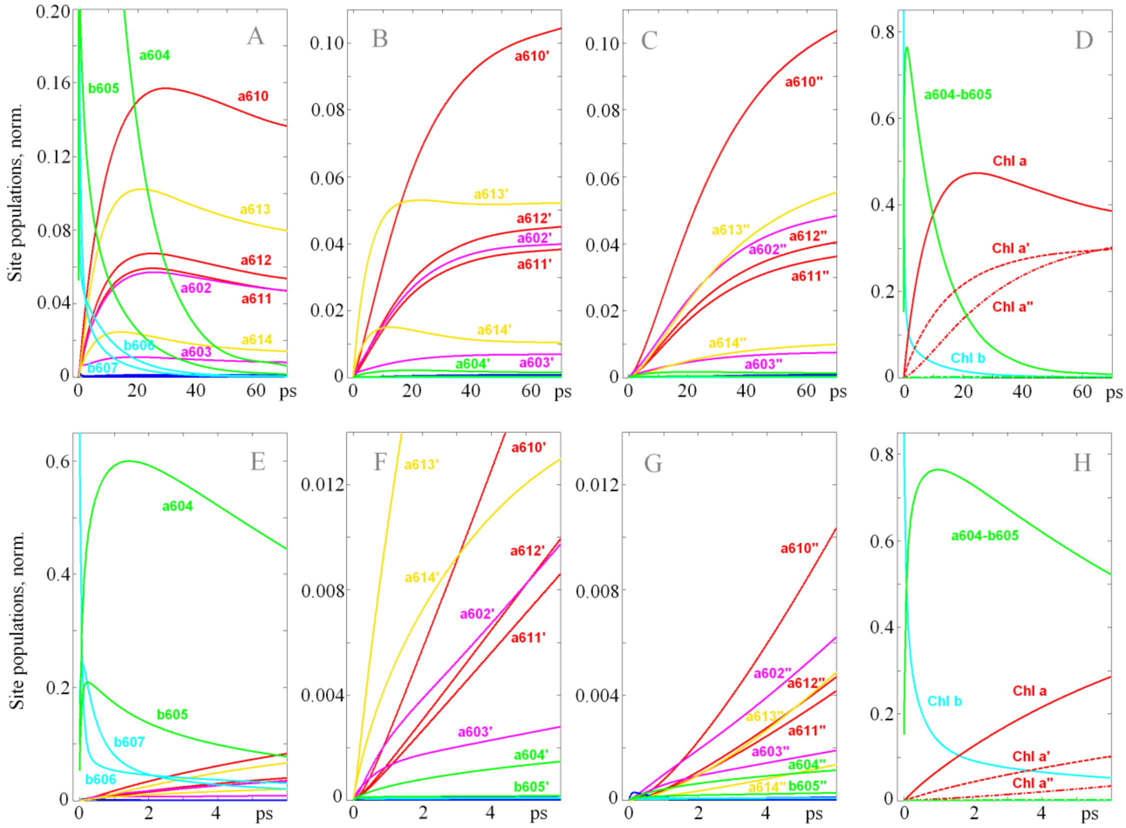

Figure S3. The same as in Figure 7, but for *b*606 initially excited (with the averaged initial values of about 0.66, 0.24, and 0.11, for *b*606, *b*607, and *b*605-*a*604 sites, respectively).

Initial excitation of *b*606 results in sub-ps equilibration within the *a*604-*b*605-606-607 cluster with predominant population of the *a*604 site (Figure S3). The following dynamics is determined by competition between the slow depopulation of the *a*604 'bottleneck' and the subsequent Chl *a*→ Chl *a*', Chl *a*" inter-monomeric equilibration. The Chl's *a* of the first subunit become populated initially during 25-30 ps (corresponding to the almost complete (90%) decay of *a*604). This is followed by a slower depopulation of Chls *a* (as shown in Figure S3A) due to transfers to Chls *a*' and Chls *a*". Figure S3D shows that the rise in Chls *a* population during 0-25 fs is faster than equilibration between Chls *a*, *a*', and *a*" after 25 ps. Thus, inter-monomeric equilibration is slower.

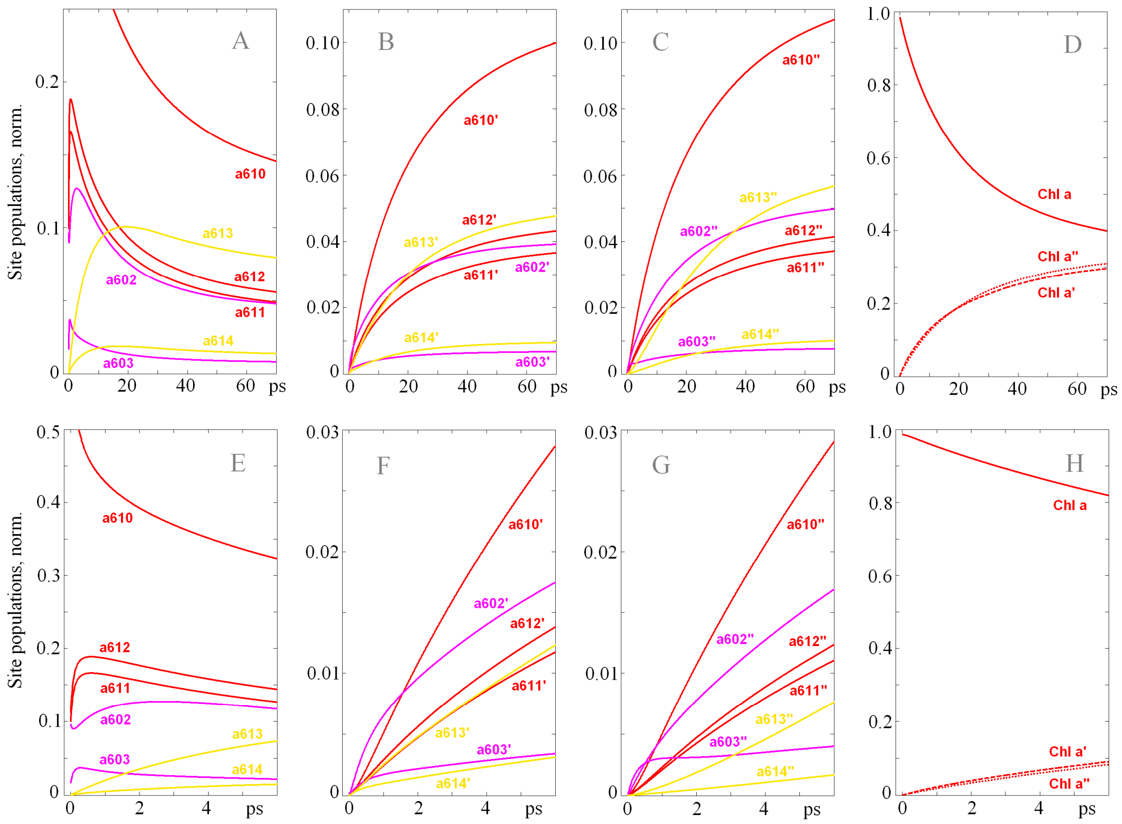

Figure S4. The same as in Figure 7, but with predominant excitation of *a*610 (with the averaged initial values of 0.67, 0.21, and 0.12 for the *a*610, *a*612-*a*611 and *a*602-603 sites).

Excitation of the red-most pigment *a*610 is followed by intra-monomeric equilibration, including (i) sub-ps equilibration within the *a*610-611-612 cluster (see fast rise in *a*611-612 populations during 0.5 ps shown in Figure S4E), (ii) equilibration with the *a*602-603 dimer with time constants of 5.5 ps ($k2_1 \rightarrow k1_1$) and 1 ps ($k2_2 \rightarrow k1_1$), and (iii) slow population of the luminal-side dimer *a*613-614 within 20 ps (see Figure S4A). Inter-monomeric transfers produce almost equal population of the second and third subunits on a time scale of several tens of ps. Initially (during 10-15 ps) the transfer to the second subunit is slightly (10%) better due to the relatively fast (6 ps) *a*603→*a*602' channel (compare the dynamics of the *a*602' and *a*602'' sites in Figure S4F,G and total Chl *a*' and *a*'' populations in Figure S4H). At larger delays (after 15-20 ps) the population of the third subunit becomes a bit faster due to the 16 ps *a*602→*a*603'' transfers (compare the *a*602' and *a*602'' dynamics in Figure S4B,C and Chl *a*'/*a*'' populations in Figure S4D).

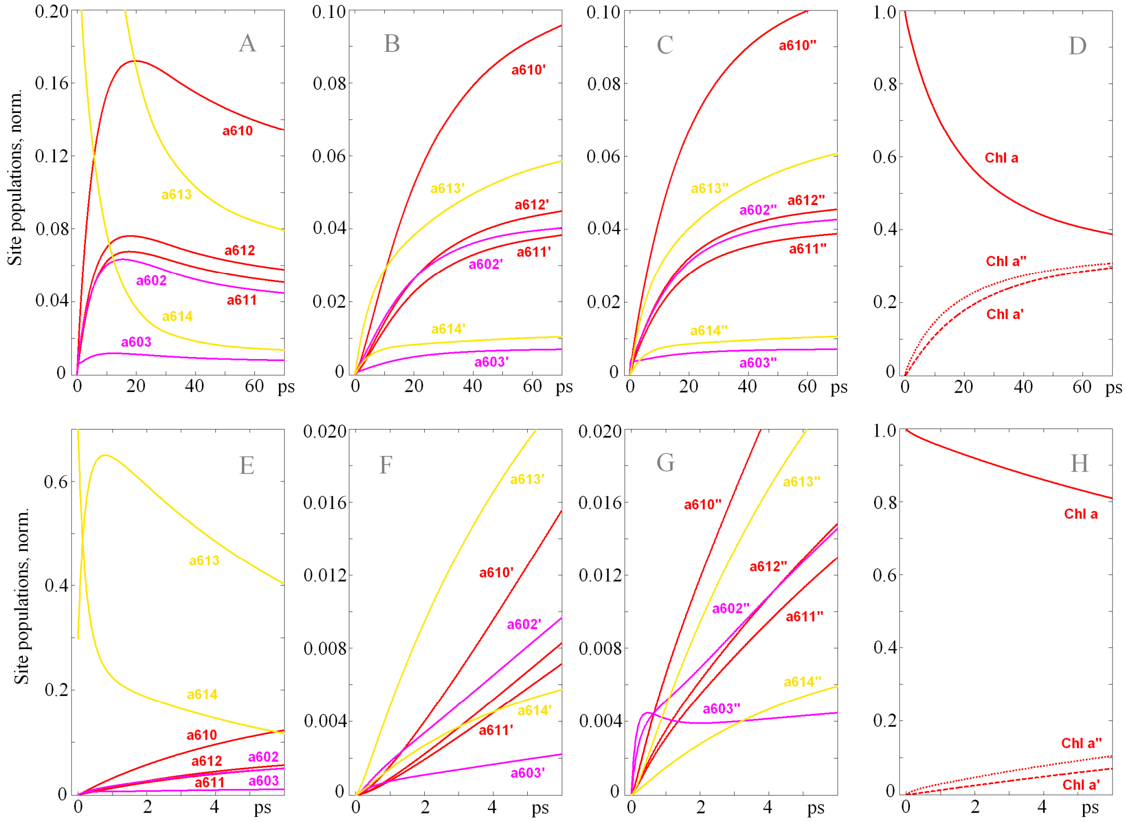

Figure S5. The same as in Figure 7, but with predominant excitation of *a*614 (with the averaged initial values of 0.7, and 0.3 for the *a*614 and *a*613 sites).

Excitation of the upper level of the *a*613-614 dimer (with predominant contribution of *a*614) results in fast (sub-ps) intra-dimer relaxation with quick depopulation of *a*614 and population of *a*613 (Figure S5E) followed by slower transfers to the stromal-side Chl's *a* within 15-20 ps (Figure S5A). After 20 ps all the populations within the first subunit decay due to slow transfers to other subunits.

The second and third subunits are again populated with a time constant of about 20 ps. Notice the small but fast populating of the third subunit (see Figure S5D,H) due to *a*614→*a*603" transfers during the short lifetime of a614 (see quick rise of *a*603" population with respect to other pigments in Figure S5G).